

Gain evaluation of Silica based Thulium doped fibre amplifier with triple pump 1050 nm+1400 nm+800 nm configuration for different values of doping concentration and doping radius

RAJANDEEP SINGH*, MANINDER LAL SINGH^{a,*}

Department of ECE GNDU RC, Fattu Dhinga (Sultanpur Lodhi), India

^aDepartment of Electronics Technology, GNDU Amritsar, India

In this paper the gain of Silica based Thulium doped fibre amplifier (TDFA) for different values of doping concentrations and doping radius has evaluated. The considered doping radius range is from 0.3 μm to 1.3 μm with an increment of 0.2 μm and the doping concentration range is from 20ppm to 140ppm with an increment of 20 ppm. In all considered cases, the best and almost similar performance has been achieved for 20ppm doping concentration with 0.9 μm doping radius and for 60 ppm doping concentration with 0.5 μm doping radius. The gain as high as 17.71dB has been obtained at 1470nm for 60 ppm doping concentration and 0.5 μm doping radius.

(Received February 28, 2016; accepted September 29, 2016)

Keywords: S-Band, TDFA, Silica, Gain, Doping concentration, Doping radius

1. Introduction

TDFA is the promising candidate for S-Band wideband optical amplification, due to low phonon energy of thulium in fluoride host, fluoride based TDFA provide better gains at relatively lower pump power [1]. But silica based TDFA has a few advantages over the fluoride based TDFA, as the silica based amplifiers are easy to splice with the standard single mode fibre, nontoxic and relatively easy to manufacture [2]. Silica host based TDFA do not provide high gain at lower pump powers due to high phonon energy [3]. In silica based TDFA, the gain can be improved by analyzing the effect of various parameters. In literature, silica based TDFA with various pumping techniques have been presented. P. Peterka et. al. presented the detailed mathematical modelling of silica based TDFA pumped with 1064nm pump [4]. P. R. Watekar et. al. presented small signal model of silica TDFA pumped with 1064 nm [2, 5]. W. Blanc, et. al. have presented experimentally and numerically the Characterization of a thulium-doped silica-based optical fibre for S-band amplification using single pump at 1060nm [6]. J. C. R. F. De Oliveira et. al presented the dual pumping techniques by using 1058 pump along with 980nm and 1047nm pumps as complimentary pumps [7]. Also, there is an approach with triple pumping of 1050nm+ 1400nm+800nm [8]. The gain characteristics of TDFA depends on many factors like pumping wavelengths, pumping powers, doping concentration, doping radius, etc. So there is a need to observe the effect of these factors on the gain characteristics of TDFA. The aim of this paper is to observe the effect of varied doping radius and doping concentration on the gain characteristics

in silica TDFA with triple pumping by using 1050nm, 1400nm and 800nm wavelengths. In this paper, the gain performance of TDFA has been evaluated for 20,40,60,80,100 and 120ppm value of Thulium doping concentration. For each doping concentration value, the gain characteristics have been plotted for different doping radius using Optisystem13.0 and Matlab software.

2. Theory

This paper is based on the model presented by P. Peterka et.al [4]. The energy level diagram of thulium ions in silica host with the triple pumping has been displayed in Fig. 1.

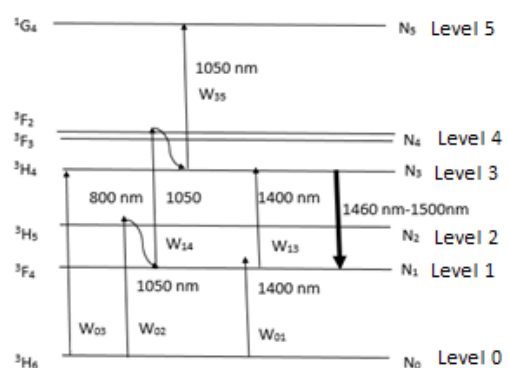


Fig. 1. Energy level diagram for triple pumping

For simplicity the $^3\text{H}_6$, $^3\text{F}_4$, $^3\text{H}_5$, $^3\text{H}_4$, $^1\text{G}_4$ energy levels are numbered as 0,1,2,3,5 respectively. Because of very

small energy differences the 3F_2 and 3F_3 levels are assumed as single level labeled as level 4. The population at level 2 and 4 is neglected due to their high decay rates. The electrons excite from ground level 0 to level 2 by absorption of 1050nm pump. Due to the very low lifetime of electrons in level 2 they quickly get migrated by non-radiative emission to level 1 from which electrons get raised to level 4 by absorbing 1050nm pump. The lifetime of an electron at level 4 is very low so the electrons quickly move to immediately lower level 3. A few electrons get upraised to level 5 from 3 level by absorption of 1050 nm pump, but they eventually returned to 3H_4 level by non-radiative emission. Similarly the absorption of 800nm pump results in the migration of electrons from ground level to level 3 directly. The 1400nm pump upraised electrons from level 0 to level 1 and then from level 1 to level 3. In this way, all the three pumps create a population inversion by shifting electrons to level 3. The rate equation for the population in Thulium doped fiber can be written as [4]

$$\begin{aligned} \frac{dN_1}{dt} &= N_0.(W_{01} + W_{02}) - N_1.(W_{10} + W_{13} + W_{14} + A_{nr1} + A_{10}) + N_3.(W_{31} + W_{32} + A_{nr3} + A_{32}) + N_5.(A_{51} + A_{52}) \\ \frac{dN_3}{dt} &= N_0.(W_{03}) + N_1.(W_{13} + W_{14}) - N_3.(W_{35} + W_{32} + W_{31} + W_{30} + A_{nr1} + A_{32} + A_{31} + A_{30}) + N_5.(A_{nr5} + A_{54} + A_{53}) \\ \frac{dN_5}{dt} &= N_0.(W_{05}) + N_3.(W_{35}) - N_5.(W_{50} + A_{nr5} + A_{54} + A_{53} + A_{52} + A_{50}) \\ \text{And } N_t &= N_0 + N_1 + N_3 + N_5 \end{aligned}$$

Where N_t is total electron density and the parameters N_0, N_1, N_3, N_5 , are the population densities of $^3H_6, ^3F_4, ^3H_4, ^1G^4$ levels respectively, W_{ij} is the stimulated absorption and emission rates from i level to j level. The radiative and non-radiative decay rates are symbolized by A_{ij} and A_{nrj} respectively the values of radiative and non-radiative lifetimes along with other parameters are given in Table 1.

Table 1. Simulation parameters

Parameter	Value	Units
Length	8.1	m
Numerical aperture	0.3	-
Core Radius	1.3	μm
Core doping radius	0.3-1.3	μm
Non radiative lifetime 1	0.00043	Seconds
Non radiative lifetime 3	45.01e-006	Seconds
Non radiative lifetime 5	0.000784	Seconds
Ar10	285.7	1/seconds
Ar30	1353.85	1/seconds
Ar31	138.46	1/seconds
Ar32	46.153	1/seconds
Ar50	581.4	1/seconds
Ar51	69.767	1/seconds
Ar52	348.84	1/seconds
Ar53	127.91	1/seconds
Ar54	34.883	1/seconds

It has been assumed that the thulium ions are excited homogeneously across the fiber cross-section, the transition rates W_{ij} can be defined by

$$W_{ij}(z) = \int_0^\infty \frac{\sigma_v(v)}{h \cdot v} \cdot I(z, v) \cdot dv$$

Where $I(z, v) = i(r, \phi, v) \cdot P_k(z)$ [4]

Where h is the Planck constant, v is the frequency, σ_v is the transition cross-section and I is the light intensity distribution.

The normalized optical intensity is defined as P_k for the k th beam

$$\begin{aligned} \frac{dP_k}{dz} &= u_k \cdot P_k(z) \cdot \sum_{ij}^{(10,30,31,50)} \int_0^{2\pi} \int_0^\infty (\sigma_{ij}(v_k) \cdot N_i(r, \phi, z) - \sigma_{ji}(v_k) \cdot N_j(r, \phi, z)) \cdot i_k(r, \phi) \cdot r \cdot dr \cdot d\phi - \\ &u_k \cdot P_k(z) \cdot \sum_{ij}^{(02,14,35)} \int_0^{2\pi} \int_0^\infty (\sigma_{ji}(v_k) \cdot N_i(r, \phi, z)) \cdot i_k(r, \phi) \cdot r \cdot dr \cdot d\phi + \\ &u_k \cdot P_{0k} \sum_{ij}^{(10,30,31,50)} \int_0^{2\pi} \int_0^\infty (\sigma_{ij}(v_k) \cdot N_i(r, \phi, z) \cdot i_k(r, \phi) \cdot r \cdot dr \cdot d\phi - \alpha(v_k) \cdot u_k \cdot P_k(z)) \end{aligned}$$

Where $u_k=+1$ for forward propagating waves and $u_k=-1$ for backward propagating waves, P_{0k} means the spontaneous emission contribution from the local population N_i .

And

$$W_{ij}(z) = \int_0^\infty \lambda \Gamma(\lambda) \cdot \sigma_{ij}(\lambda) \frac{(P_\lambda^+(z, \lambda) + P_\lambda^-(z, \lambda))}{hc\pi b^2} d\lambda$$

$$\text{where } \Gamma(\lambda) = \frac{\int_0^\infty |E(r, \phi, \lambda)|^2 N(r) \cdot r \cdot dr}{N_t \int_0^\infty |E(r, \phi, \lambda)|^2 \cdot r \cdot dr}$$

The propagation equation of the beams through the doped fiber is given by

$$\begin{aligned} \frac{dP^+(\lambda)}{dz} &= \Gamma(\lambda) \cdot P^+(\lambda) \cdot \sum_{ij}^{(10,30,31,50,32)} (N_i \cdot \sigma_{ij}(\lambda) - N_j \cdot \sigma_{ji}(\lambda)) - \\ &\Gamma(\lambda) \cdot P^+(\lambda) \cdot (N_0 \cdot \sigma_{02}(\lambda) + N_1 \cdot \sigma_{14}(\lambda) + N_3 \cdot \sigma_{35}(\lambda)) + \\ &\Gamma(\lambda) \cdot \sum_{ij}^{(10,30,31,50,32)} 2hv_{ij} \Delta v N_i \cdot \sigma_{ij}(\lambda) - \alpha(\lambda) \cdot P^+(\lambda) \end{aligned}$$

By setting the time derivatives $\frac{dN_1}{dt}$, $\frac{dN_3}{dt}$, $\frac{dN_5}{dt}$ to zero, the problem is reduced to the steady-state case. With the specified boundary conditions at $z = 0$ and $z = L$ the equations are integrated over space, and frequency, from the input power and output power gain is obtained.

3. Simulation setup

Fig. 2 shows the simulation setup used, in the transmitter section a continuous wave laser array of 20 lasers with -20dB power each, with the wavelength ranging from 1450 nm to 1520 nm, having wavelength spacing of 5 nm have been placed. The power of each laser is fixed at -20dB. All the signal wavelengths are multiplexed together using a multiplexer, the multiplexed signal is the combined with the co-propagating pump

signal of 1050nm having 1000mW power. The signal is then fed to the silica-based thulium doped fibre amplifier. From counter-propagating direction two pumps of 1400nm and 800nm having 300mW power each combined together are fed to the thulium doped fibre amplifier.

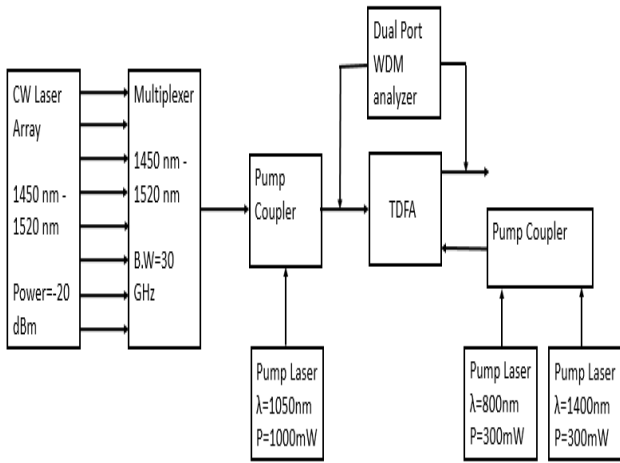


Fig. 2. Simulation setup

In the simulation setup TDFA length of 8.1m, core radius has been fixed to 1.3 micro meters throughout the paper. Table 1 shows the parameters used in the simulation. Gain has been observed with the help of dual port WDM analyzer.

4. Results and discussion

Fig. 3 shows the gain vs wavelength for 20 ppm doping and varied doping radius, the figure shows that the maximum gain is obtained at the doping radius of 0.9µm. The maximum gain of 16 dB has been obtained at 1470nm, TDFA provides positive gain till 1510nm wavelength, at 1520nm only 0.3 µm and 0.5 µm doping radius provides positive gain.

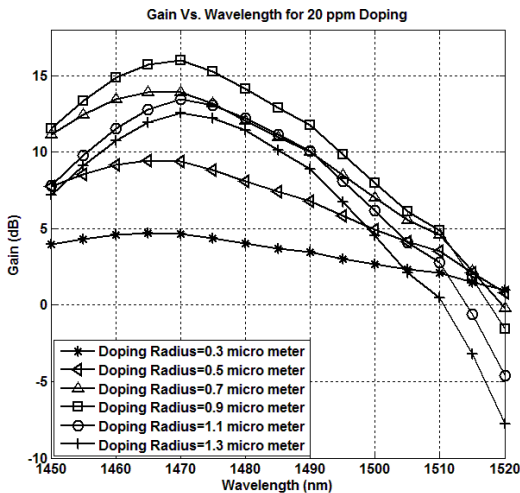


Fig. 3. Gain vs. Wavelength for 20 ppm doping

Fig. 4 is the graphical representation of gain for 40ppm TDFA concentration, the maximum gain has been observed for doping radius 0.5 µm in region 1450nm to 1500 nm. The gain decreases more sharply at higher wavelengths in the 40ppm case when compared to the 20ppm doping concentration, maximum gain of 15.02dB has been observed at 1470nm for 0.5 µm. In Fig. 5 and 6, Gain vs. Wavelength has been plotted for 60 ppm and 80ppm doping respectively. For 60 ppm doping concentration, the maximum gain is observed at the doping radius of 0.7µm, the maximum gain obtained is 17.98dB at 1470nm, and 4.9dB at 1510nm.

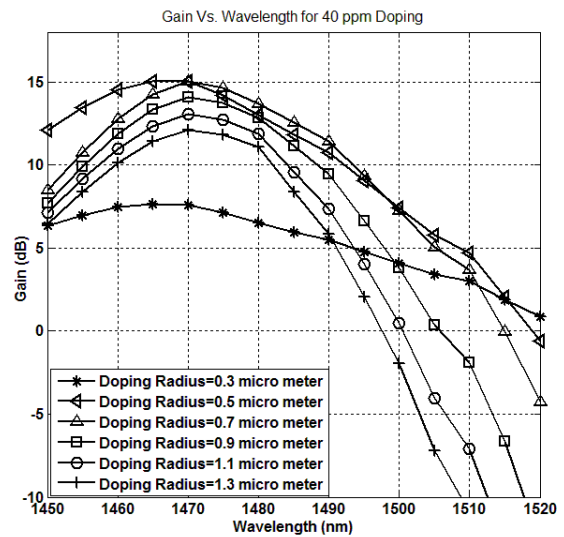


Fig. 4. Gain vs. Wavelength for 40 ppm doping

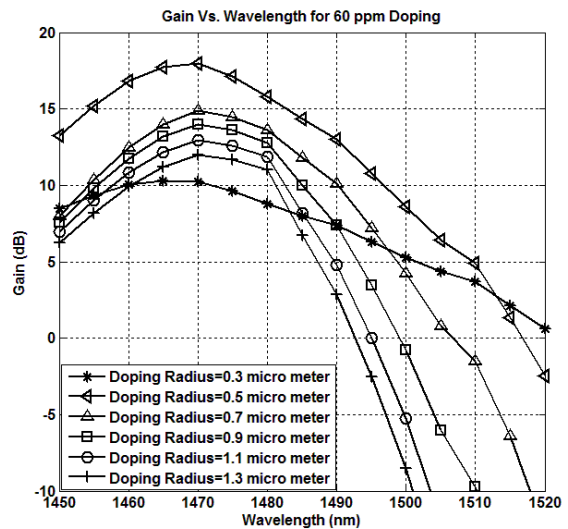


Fig. 5. Gain vs. Wavelength for 60 ppm doping

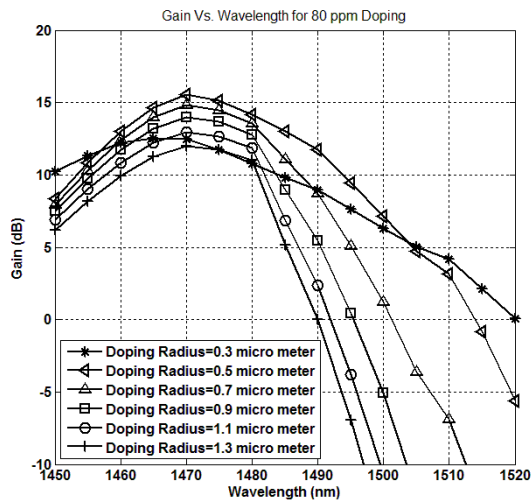


Fig. 6. Gain vs. Wavelength for 80 ppm doping

In case of 80ppm doping concentration, 0.5 μm doping radius provides the best gain of 15.6 dB at 1470 nm, But at 1510nm gain for all the doping radius values is negative.

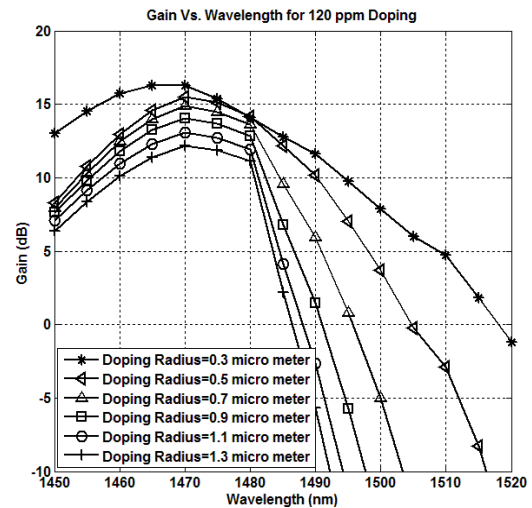


Fig. 8. Gain vs. Wavelength for 120 ppm doping

In 120ppm doping radius case the doping radius value of 0.3 μm comes out as best performing case, the gain of 13.03dB at 1450, 16.30dB at 1470nm and 5 dB at 1510nm has been observed.

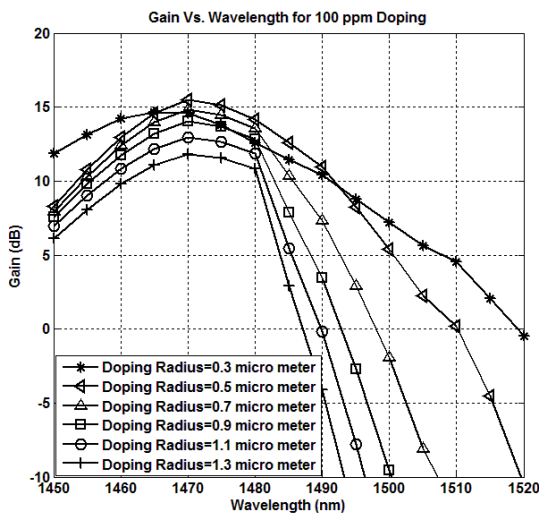


Fig. 7. Gain vs. Wavelength for 100 ppm doping

Gain vs. Wavelength characteristics for 100 ppm and 120 ppm doping have been shown in Fig. 7 and 8 respectively. From these figures, it has been observed that gain at the higher wavelengths decreases sharply as the doping concentration increases. At 1450nm and 1470nm the maximum gains of 14.19dB and 14.58dB respectively have been obtained in the case of 100ppm doping for doping radius 0.3 μm , and the positive gain extends up to 1500nm. The most flatten gain curve has been observed for 0.3 μm doping concentration but the maximum gain of 14.62dB has been obtained at 1470nm for 0.5 μm doping radius.

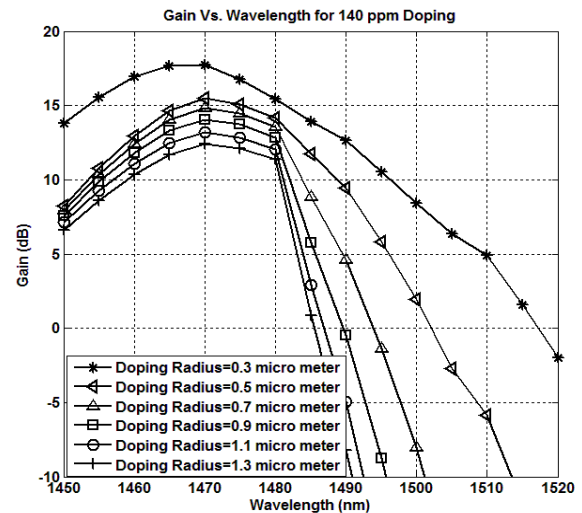


Fig. 9. Gain vs. Wavelength for 140 ppm doping

Fig. 9 shows the gain characteristics for 140ppm doping concentration, the best results have been observed for doping radius value of 0.3 μm . The gain of 16.95dB has been observed at 1450nm, 17.71dB at 1470nm and 5 dB at 1510nm has been observed.

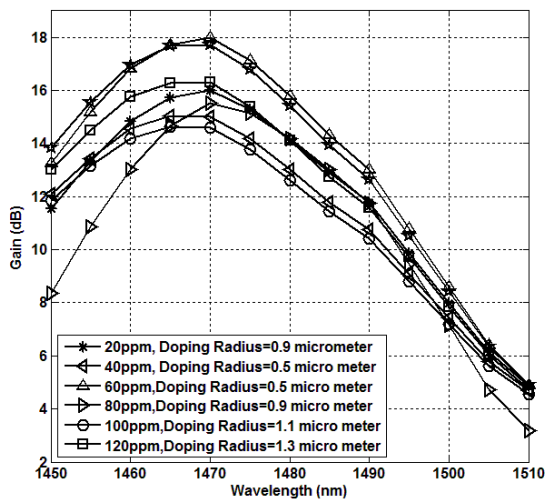


Fig. 10. Best Gain vs. Wavelength characteristics

Fig. 10 shows best gain characteristics from each case of doping concentration i.e. 20 ppm to 140ppm. From the figure it has been observed that the best and almost same gain has been provided by two cases which are 20ppm with $0.3\mu\text{m}$ doping radius and 60 ppm doping concentration with $0.5\mu\text{m}$ doping radius, in both cases, the gain is around 14 dB at 1460nm and 17.7dB at 1470nm.

5. Conclusion

In this paper, the gain characteristics of silica TDFA for S-Band systems have been analyzed for varied doping radius from $0.3\mu\text{m}$ to $1.3\mu\text{m}$ and doping concentration from 20ppm to 140ppm. From the results it has been observed that the doping radius is an important parameter of TDFA, The different combinations of the doping radius and doping concentration have been tried to find the optimum results. It is concluded that with the increase in both doping concentration and doping radius, the gain at higher wavelengths decreases very sharply. The best and almost similar results have been obtained for 20ppm doping concentration with $0.9\mu\text{m}$ doping radius and 60 ppm doping concentration with $0.5\mu\text{m}$ doping radius. In both cases the cases the gain is close to 14 dB at 1460nm, the maximum of 17.71dB at 1470nm has been achieved by 60 ppm doping concentration with $0.5\mu\text{m}$ doping radius.

References

- [1] M. Eichhorn, IEEE Journal of Quantum Electronics **41**(12), 1574 (2005).
- [2] P. R. Watekar, Seongmin Ju, Won-Taek Han, in Photonics Technology Letters, IEEE **8**(19), 2035 (2006).
- [3] K. P. W. Dissanayake, S. D. Emami, H. A. Abdul-Rashidi, S. M. Aljamimi, Z. Yusoff, M. I. Zulkifli, S. Z. Muhamad-Yassin, K. A. Mat-Sharif, N. Tamchek, IEEE 4th International Conference on Photonics (ICP), **28-30**, 288 (2013).
- [4] P. Peterka, B. Faure, W. Blanc, M. Karásek, B. Dussardier, Optical and Quantum Electronics **36**(13), 201 (2004).
- [5] P. R. Watekar, S. Ju, W. T. Han, J. Light. Technol. **25**(4), 1045 (2007).
- [6] W. Blanc, et al, Proceedings of SPIE, International Society for Optical Engineering, **6180**, 61800V.1 (2006).
- [7] J. C. R. F. De Oliveira, J. B. Rosolem, A. A. Juriollo, Proc. 2003 SBMO/IEEE MTT-S Int. Microw. Optoelectron. Conf. – IMOC **1**, 235 (2003).
- [8] Rajandeep Singh, Maninder Lal Singh, Baljeet Kaur, Optik - International Journal for Light and Electron Optics **123**(20), 1815 (2012).

*Corresponding author: rajandeep.ecespl@gndu.ac.in, mlsingh7@gmail.com